Dissociative electron attachment and vibrational excitation of the chlorine molecule

Přemysl Kolorenč and Jiří Horáček
Institute of Theoretical Physics, Faculty of Mathematics and Physics, Charles University in Prague, Prague, Czech Republic
(Received 24 May 2006; published 6 December 2006)

This paper is aimed at the theoretical investigation of the inelastic processes taking place in resonant collisions of low-energy electrons with the chlorine molecule. Dissociative electron attachment and vibrational excitation of Cl_2 by electron impact is investigated in the energy range 0–1.5 eV, where the $^2\Sigma_u^+$ resonance plays the central role. The calculations were carried out within the framework of the nonlocal resonance model. This approach makes it possible to calculate the integrated cross sections of the above-mentioned processes for a variety of initial and final rovibrational states of the target molecule. The present model is constructed on the basis of *ab initio* fixed-nuclei *R*-matrix calculations using the so-called Feshbach-Fano *R*-matrix method. The Schwinger-Lanczos algorithm was utilized to solve the Lippmann-Schwinger equation describing the motion of the nuclei.

DOI: 10.1103/PhysRevA.74.062703 PACS number(s): 34.80.Ht, 34.50.Ez, 31.15.Ar

I. INTRODUCTION

Molecular chlorine is an important gas in plasma processing (the Cl atoms produced in a gas discharge efficiently etch the silicon surface) or in excimer lasers. It is also of atmospheric and environmental interest. A comprehensive review of available data on a broad variety of processes taking place in electron-Cl_2 collisions, including dissociative electron attachment (DEA), was published by Christophorou and Olthoff [1]. In the past the DEA cross section was measured in three electron-beam experiments carried out by Tam and Wong [2], by Kurepa and Belić [3], and by Azria *et al.* [4]. All those experiments found a peak in the cross sections at zero energy, which is in direct contradiction with the general theory of *p*-wave scattering (at the lowest energies the DEA process is dominated by the $^2\Sigma_u^+$ resonance and the zero angular momentum of the incoming electron does not contribute to this symmetry), which predicts the threshold behavior $\sigma_{\mathrm{DEA}} \propto \epsilon^{1/2}$. Only the measurement of Kurepa and Belić provides the absolute values of the cross section. Another absolute measurement of the process is the swarm-type experiment of McCorkle *et al.* [5] in which the nonequilibrium DEA rate constants were acquired as a function of mean electron energy.

More recently, the shape of the cross section was remeasured by Hotop and co-workers [6,7]. This experiment found the "zero-energy peak" to be shifted to the collision energy of about 60 meV and revealed the threshold behavior predicted by the theory. These results are in excellent agreement with the only calculations of the DEA via the $^2\Sigma_u^+$ resonance in electron-Cl_2 collisions carried out by Fabrikant *et al.* [8]. These calculations are based on semiempirical *R*-matrix theory, in which the usual *R*-matrix expansion is approximated by a single term. Its pole (which corresponds to some extent to the diabatic curve used in the nonlocal resonance model described later) can be determined as a position of the resonance in fixed-nuclei (FN) electron scattering. The surface amplitude is parametrized analytically and fitted to reproduce experimental data, in the case of Ref. [8] the DEA cross sections of Kurepa and Belić [3]. In Ref. [7], the model is extended for electron energies up to 9 eV by inclusion of the $^2\Pi_g$ and $^2\Pi_u$ resonances into the theoretical description of the collisions. This model is also used to predict the cross sections of the process of vibrational excitation (VE) by electron impact [7]. The calculation represents the only available data on the VE cross section, since there is no direct measurement of the process. Only rough estimates of the total VE cross section derived from the difference of the total inelastic electron scattering cross section and the total ionization and dissociation cross sections, for which experimental data are available, are provided by Christophorou and Olthoff [1]. Other predictions have been made on the basis of Boltzmann-code calculations using limited data from swarm experiments [9,10].

In this paper we present a fully *ab initio* calculation of the processes of DEA and VE of the Cl_2 molecule. Our approach is based on the nonlocal resonance model (NRM) [11], which provides the most comprehensive theory of resonant nuclear dynamics, describing at least qualitatively all the experimentally observed features [12–14]. The theory of the NRM makes use of the Feshbach-Fano projection-operator formalism [15–17] originally developed in nuclear physics to exploit the advantages of partitioning the total wave function into closed- and open-channel segments. The resonance is represented by a square integrable wave function (the discrete state) which interacts with the continuum of background scattering states. Once the the discrete state, its energy, and the coupling elements are known, the cross sections of different inelastic processes taking place in the low-energy resonant electron-molecule collisions can be evaluated ([18–20], and references therein).

In the past, several *ab initio* techniques have been utilized to construct the NRM for diatomic molecules, from fitting analytical formulas for the discrete-state potential and resonance width functions to the fixed-nuclei phase shifts (without direct consideration of the discrete state wave function) [21] to more elaborate methods based on the Stieltjes moment theory [22,23] or the many-body optical-potential approach [24]. In the present work we applied the Feshbach-Fano *R*-matrix (FFR) method [20,25]. In this approach the discrete state, its energy, and the corresponding coupling terms with the scattering continuum, as well as the back-

ground scattering eigenphases, are extracted from *ab initio* fixed-nuclei *R*-matrix calculations. In the last few years the method was used to examine resonances in several molecules [25–28]. In combination with the theory of the NRM the method was first used by Brems *et al.* [29] to study the problem of DEA and VE of the fluorine molecule.

The paper is organized as follows. In Sec. II, the theory of the NRM is briefly reviewed, followed by a short description of the *R*-matrix theory and the FFR method. In Sec. III the results of the FN calculations are summarized and the construction of the NRM is described. Final results for the cross sections of the processes of DEA and VE are collected and compared with other available experimental and theoretical data in Secs. IV and V. The paper is summarized in Sec. VI.

II. THEORY

A. Nonlocal resonance model

In low-energy electron-molecule collisions, a variety of inelastic and reactive processes take place, such as the above-mentioned vibrational excitation or dissociative electron attachment. Direct energy transfer between the electron and the nuclei is usually ineffective and the contribution of direct scattering to these processes is negligible. In many diatomic molecules, however, the efficiency of the inelastic processes is enhanced by formation of an unstable negative molecular ion during the collision. In such a case, the processes proceed according to the scheme

$$\begin{array}{lcll} & & & e^- + AB(\nu',J') \\ e^- + AB(\nu,J) & & & \\ & \rightarrow\ (AB)^-\ \rightarrow & A + B^- & \\ A + B^- & & & \\ & & & A + B + e^-, \end{array} \tag{1}$$

where A and B substitute two arbitrary atoms. In the nonlocal resonance theory, the metastable molecular anionic state $(AB)^-$ is represented by a square integrable wave function, the discrete state $|\varphi_d\rangle$. This state interacts with the background scattering continuum via the matrix elements $V_{d\epsilon}(R)$, where R is the internuclear distance. When the incoming electron is temporarily bound to the molecule the nuclei start to move on the discrete-state potential $V_d(R)$ (which is usually dissociative for the lowest resonance states) toward larger internuclear distances. At any time the electron can autodetach, leaving the molecule in a possibly vibrationally excited state. If, however, the complex $(AB)^-$ reaches the crossing of $V_d(R)$ with the potential $V_0(R)$ of the neutral molecule the molecular ion becomes electronically stable (bound state) and the process of DEA is completed.

The motion of the nuclei is described by the Lippmann-Schwinger equation

$$|\Psi^{(+)}\rangle = |\Phi^{(+)}\rangle + G_Q^{(+)}(E)F(E)|\Psi^{(+)}\rangle, \tag{2}$$

where $G_Q^{(+)}(E)$ is the Green's function corresponding to the Hamiltonian $H_Q = T_N + V_d$. Apart from the local long-range discrete-state potential $V_d(R)$ another interaction appears in Eq. (2), which is described by the short-range, complex, and energy-dependent operator

$$\langle R'|F(E)|R\rangle = \int d\vec{\epsilon} V_{d\vec{\epsilon}}(R')[E - T_N - V_0(R) - \epsilon + i\eta]^{-1} V^*_{d\vec{\epsilon}}(R). \tag{3}$$

T_N is the operator of the nuclear kinetic energy. The principal advantage of the approach is that the electronic degrees of freedom are projected out and we are left with an effective two-body problem which can be solved very efficiently, usually in a partial wave expansion. The many-body character of the collision is reflected by the nonlocality and energy dependence of the interaction.

In the case of VE the boundary condition for Eq. (2) is $|\Phi^{(+)}\rangle = G_Q^{(+)}(E)V_{d\epsilon_i}|\zeta_i\rangle$, where $|\zeta_i\rangle$ is the wave function of the initial state of the target molecule and ϵ_i is the energy of the incoming electron. The formula for the T matrix then reads

$$T_{\mathrm{VE}}(\zeta_i, \zeta_f, \epsilon_i) = \langle \zeta_f | V^*_{d\epsilon_i} | \Psi^{(+)} \rangle. \tag{4}$$

For the process of DEA the proper boundary condition in Eq. (2) is the scattering solution for the Hamiltonian H_Q for the energy E, $|\Phi^{(+)}\rangle = |E^{(+)}\rangle$. For the T matrix we obtain the formula

$$T_{\mathrm{DEA}}(\zeta_i, \epsilon_i) = \langle \Psi^{(-)} | V_{d\epsilon_i} | \zeta_i \rangle. \tag{5}$$

B. Feshbach-Fano *R*-matrix method

In this section we will briefly discuss how the discrete state $|\varphi_d\rangle$ may be defined in the framework of the *R*-matrix theory. A detailed derivation of the FFR method may be found in Refs. [25,30]. The fundamental idea of the *R*-matrix theory [31] is to divide the configuration space into two regions by a sphere Ω centered on the target. The radius r_Ω of the sphere is chosen such that outside the sphere (*external region*) the electron-target interaction can be approximated by an effective single-particle potential (usually in a multipole expansion). Inside the sphere (*internal region*), on the other hand, electron exchange and correlation between the target and scattered electron have to be taken into account. If the $(N+1)$-electron Hamiltonian (N is the number of electrons of the neutral molecule)

$$H_{N+1} = \sum_{i=1}^{N+1} \left(-\frac{1}{2}\Delta_i - \frac{Z_A}{r_{Ai}} - \frac{Z_B}{r_{Bi}} \right) + \frac{Z_A Z_B}{R} + \sum_{i>j=1}^{N} \frac{1}{r_{ij}} \tag{6}$$

is modified by adding the Bloch operator $L^\Omega_{N+1} = \frac{1}{2}\Sigma_{i=1}^{N+1} \delta(r_i - r_\Omega) d/dr_i$ (see Ref. [32]) we obtain an operator that is Hermitian in the space of functions defined in the internal region and regular at the origin. The eigenvalue problem

$$H^\Omega_{N+1}|\Psi^\Omega_k\rangle = (H_{N+1} + L^\Omega_{N+1})|\Psi^\Omega_k\rangle = E^\Omega_k|\Psi^\Omega_k\rangle \tag{7}$$

provides a discretization of the scattering continuum in the internal region, resulting in real eigenvalues and orthonormal eigenfunctions. It should be stressed that the wave functions $|\Psi^\Omega_k\rangle$ are defined only inside the sphere Ω, but do not vanish at its surface, since they do not correspond to bound states.

The key role in R-matrix theory is played by the *channel surface amplitudes*

$$w_{ik} \equiv \langle \bar{\Phi}_i; r_\Omega | \Psi_k^\Omega \rangle' = \int d\mathbf{x}_1 \cdots d\mathbf{x}_{N+1} \bar{\Phi}_i(\mathbf{x}_1, \ldots, \mathbf{x}_N; \hat{r}_{N+1}\sigma_{N+1}) \frac{1}{r_{N+1}} \times \delta(r_{N+1} - r_\Omega) \Psi_k^\Omega(\mathbf{x}_1, \ldots, \mathbf{x}_{N+1}). \quad (8)$$

Here $\bar{\Phi}_i(\mathbf{x}_1, \ldots, \mathbf{x}_N; \hat{r}_{N+1}\sigma_{N+1})$ are the channel functions obtained by coupling the target states $|\Phi_i\rangle$,

$$H_N|\Phi_i\rangle = W_i|\Phi_i\rangle, \quad (9)$$

with the angular and spin functions of the scattered electron to form the eigenstates of the total angular momentum, spin, and parity [H_N is the electronic Hamiltonian of the neutral molecule, $\mathbf{x}_i$ denotes the spatial and spin coordinates $(\vec{r}_i, \sigma_i)$ of the ith electron, and $\hat{r}_{N+1}$ stands for the angular coordinates of the vector $\vec{r}_{N+1}$]. The channel surface amplitudes and the *poles* E_k^Ω can be used to construct the R matrix,

$$R_{ij}(\epsilon) = \frac{1}{2} \sum_k \frac{w_{ik} w_{jk}^*}{E_k^\Omega - \epsilon}. \quad (10)$$

The R matrix provides the boundary condition for the solution of the Schrödinger equation in the external region (where the problem reduces to the solution of coupled local differential equations) and can be therefore used to obtain all the necessary scattering quantities, such as the S matrix and eigenphases.

The R-matrix formalism can be used to construct the NRM as follows. Provided the radius r_Ω is large enough the square integrable wave function $|\varphi_d\rangle$ can be assumed to vanish outside the sphere Ω. It can thus be represented as a linear combination of the R-matrix basis functions,

$$|\varphi_d\rangle = \sum_{E_k^\Omega \in \Sigma_{\text{res}}} c_k^\Omega |\Psi_k^\Omega\rangle, \quad (11)$$

where Σ_{res} is an energy domain in which the discrete state is expected to interact with the background continuum. Equations for the expansion coefficients c_k^Ω can be found by comparison of the investigated resonant system with a similar potential (the so-called model system described by the Hamiltonian $^\circ H_{N+1}$) possessing no resonance in the energy region Σ_{res}. Usually, the Hamiltonian $H_{\text{free}} = H_N + T_{el}$ describing the neutral molecule and free electron is used, for which the the R-matrix poles and surface amplitudes can be obtained analytically using only the knowledge of the solution of Eq. (9) [25]. The key idea is that the background scattering subspace of the complete Hilbert space is represented by the eigenfunctions of the modified model Hamiltonian $^\circ H_{N+1}^\Omega$ [cf Eq. (7)]. The orthogonality of the discrete state to the background scattering subspace yields the system of linear equations for the coefficients c_k^Ω,

$$\sum_{k=1}^{N} c_k^\Omega \langle {}^\circ \Psi_j^\Omega | \Psi_k^\Omega \rangle = 0, \quad {}^\circ E_j^\Omega \in \Sigma_{\text{res}}. \quad (12)$$

When the discrete state is determined the discrete-state–continuum coupling $V_{d\epsilon}$ can be obtained by direct evaluation of the proper matrix elements of the modified Hamiltonian between the discrete state and the eigenfunctions of the background Hamiltonian $^{\text{bg}}H^\Omega = PH^\Omega P$ with $P = 1 - |\varphi_d\rangle\langle\varphi_d|$. For explicit formulas see Ref. [25]. No further approximation has to be introduced; the separation of the Hilbert space into the resonance and background scattering subspaces and their coupling are exact. The only limitations of the method originate from the expansion of the target states $|\Phi_i\rangle$ and the $(N+1)$-electron wave functions $|\Psi_k^\Omega\rangle$.

III. FIXED-NUCLEI CALCULATIONS AND CONSTRUCTION OF THE MODEL

In the present work we have used the Feshbach-Fano R-matrix method to construct the nonlocal resonance model for low-energy electron-Cl_2 scattering, driven by the lowest $^2\Sigma_u^+$ resonance. In the initial fixed-nuclei R-matrix calculations, target orbitals were constructed from the correlation-consistent polarized valence triple-zeta (cc-pVTZ) $(15s9p2d1f)/[5s4p2d1f]$ basis set of Woon and Dunning [33], centered on each of the atoms. This basis was chosen in order to meet the requirement of the R-matrix theory that the target wave function is completely contained within the sphere Ω. In the present calculations its radius was set to $r_\Omega = 10$ bohr. The scattering continuum was expanded in a diffuse basis centered on the center of mass of the molecule. It was constructed from Gaussian functions optimized in order to fit selected Bessel functions within the sphere Ω [29,34]. The molecular orbitals (MO's) were defined in two steps. First, compact MO's are defined via solution of the Hartree-Fock (HF) equations for the neutral (N-electron) system in the compact basis. Then, the continuum MO's are expanded in the complete basis (compact and diffuse functions) and orthogonalized with respect to compact orbitals obtained in the first step.

The R-matrix calculations were carried out at static-exchange (SE) and static-exchange plus polarization (SEP) levels. The SE level of computation in the Σ_u symmetry consists of expanding the $(N+1)$-electron wave function in a set of configurations defined by adding one electron into each unoccupied σ_u orbital (compact or diffuse) in the SE ground-state configuration of the neutral molecule. At the SEP level, the polarization of the target is taken into account via adding to the SE set of configurations all configurations defined by exciting a single electron from any (compact or diffuse) orbital occupied in the SE configurations into any unoccupied compact orbital. Only the lowest four eigenstates of H^Ω were determined at the SEP level of theory. Corresponding eigenvalues lie in the spectral domain 0–14 eV above the ground-state energy of the Cl_2 molecule. The R-matrix expansion was complemented by levels calculated at the SE level and orthogonalized to the lowest four SEP eigenstates. We will refer to these calculations as the SEP +SE level of theory. The FN calculations were carried out for 57 internuclear distances between 2.5 and 6.0 bohr.

In the FFR procedure, the three lowest R-matrix levels were used to expand the discrete-state wave function. As a

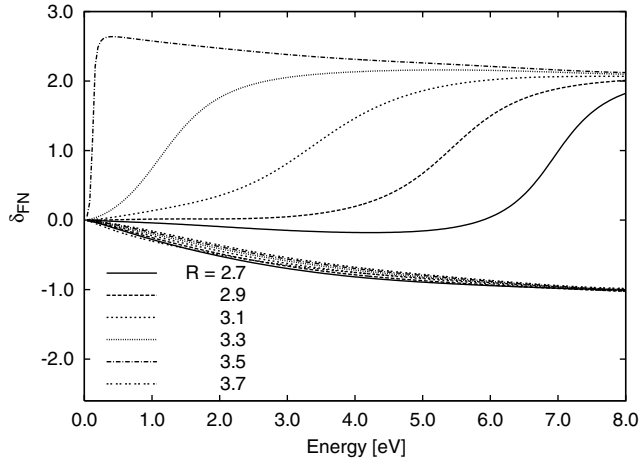

FIG. 1. Full and background (lower curves) FN eigenphase sums for electron-Cl_2 scattering. SEP+SE level, R in bohr. For $R=3.7$ bohr no resonance behavior can be observed in the full eigenphase sum (this geometry belongs to the bound-state region) and both the full and background eigenphase sums are flat.

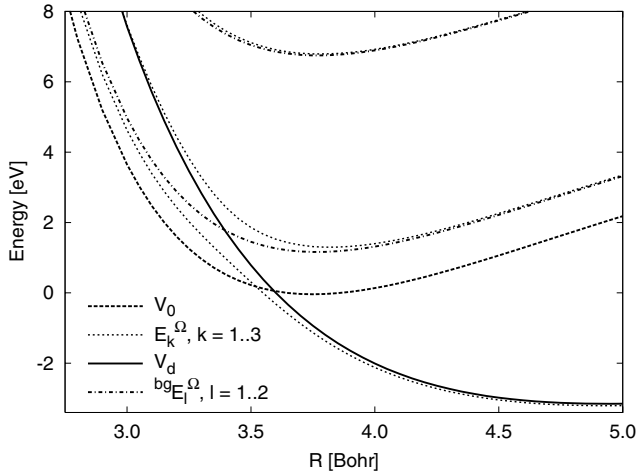

FIG. 3. Cl_2^- potential curves, SEP+SE level. The region beyond the crossing of $V_d(R)$ and $V_0(R)$ ($R>3.59$ bohr) is referred to as the bound-state region and the region of smaller R is the resonance region.

model system we have utilized the free-electron Hamiltonian H_{free}. The overlap integrals $\langle {}^{\circ}\Psi_j^{\Omega}|\Psi_k^{\Omega}\rangle$ in Eq. (12) were estimated using the Nestmann approximation (NA) method (for derivation of the approximation see Ref. [30]). In Fig. 1 the full fixed-nuclei eigenphase sum δ_{FN} is plotted for six internuclear distances. In the same figure, the lower curves correspond to the background eigenphase sum δ_{bg}, obtained after the removal of the discrete state from the electronic Hilbert space. We observe that the resonance behavior is completely removed from δ_{bg}, which becomes weakly dependent on energy and nearly independent of the molecular geometry. The fixed-nuclei width $\Gamma_{\text{FN}}(\epsilon)=2\pi|V_{d\epsilon}|^2$ is plotted in Fig. 2 as a function of electron energy for the same internuclear distances as used in Fig. 1. Note that $\Gamma_{\text{FN}}(\epsilon;R)$ does not vanish in the bound-state region ($R>3.59$ bohr; see Fig. 3) even though the eigenphase sum does not show any indication of the resonance behavior in this area. It is caused by the fact that the selected discrete state does not correspond exactly to the bound-state wave function of Cl_2^-.

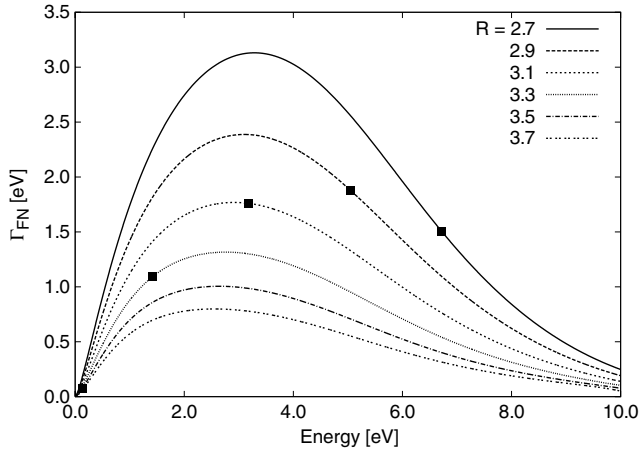

FIG. 2. Energy-dependent width function $\Gamma(\epsilon)$ for several internuclear distances. Points show the estimated local resonance positions and widths. SEP+SE level, R in bohr. Note that the resonance width function does not vanish in the bound-state region ($R=3.7$ bohr).

The Cl_2 ground-state potential energy curve $V_0(R)$ (SE level) and the lowest R-matrix poles $E_k^{\Omega}(R)$ are plotted in Fig. 3. The figure shows also the diabatized spectrum, consisting of the discrete state energy $V_d(R)$ and the background R-matrix poles ${}^{\text{bg}}E_l^{\Omega}(R)$. The equilibrium internuclear distance of the neutral molecule is 3.75 bohr. The discrete-state potential $V_d(R)$ crosses $V_0(R)$ at 3.59 bohr and has a minimum at 4.9 bohr. We will call the interval below the crossing ($R<3.59$ bohr) the *resonance region* and the region beyond the crossing the *bound-state region*.

The potential curves $V_0(R)$ and $V_d(R)$ of Fig. 3 and the resonance width function $\Gamma(\epsilon,R)\equiv\Gamma_{\text{FN}}(\epsilon;R)$ of Fig. 2 fully define the nonlocal resonance model of the ${}^2\Sigma_u^+$ resonance in electron-Cl_2 collisions. A major drawback of the SE potential curves is the incorrect trend of $V_0(R)$ for larger internuclear distances. It is caused by the wrong asymptotic behavior of the HF wave functions—in the present implementation (restricted HF) the open-shell fragments, into which Cl_2 dissociates, cannot be described properly. For the treatment of the nuclear dynamics we have improved the nonlocal resonance model in the following way. The potential energy of the neutral molecule was replaced by a curve calculated at the multireference doubly excited configuration interaction (MRD-CI) level of theory in the whole range of internuclear distances up to 20 bohr. For the discrete-state potential, the original SEP+SE data are used for $R<6$ bohr. For larger internuclear distances, $V_d(R)$ is continued by the potential energy curve of Cl_2^- calculated at the MRD-CI level. The relative position of the two curves is then determined by the accurate value for electron affinity 3.42 eV calculated by Peyerimhoff and Buenker [35]. For the resonance width the original data obtained at the SEP+SE level of theory (Fig. 2) are used in the final model; for $R>6$ bohr the resonance width vanishes. The reason why the scattering calculations

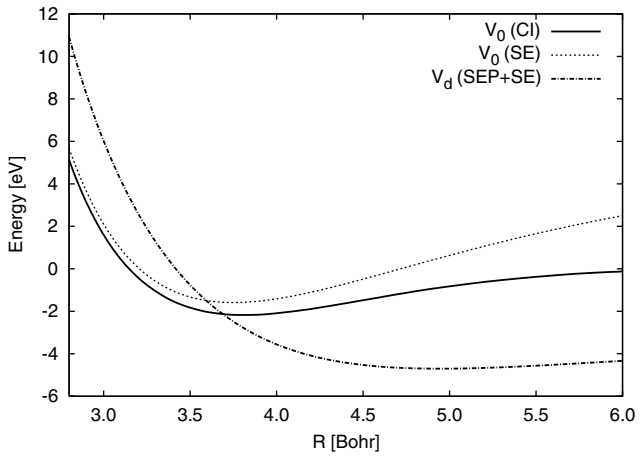

FIG. 4. Comparison of the potential curves of the original (SEP+SE level) and improved (CI for V_0 and SEP+SE for V_d in the depicted region) models. The two sets of curves are shifted so that the discrete-state potentials match in the resonance region.

were not repeated at the higher level of theory lies in the limitation of the used R-matrix codes.[1]

A comparison of the original potential curves determined at the SEP+SE level of theory (see Fig. 3) with the potential curves of the improved model [CI level for $V_0(R)$ and SEP+SE level for $V_d(R)$ in the depicted region] is shown in Fig. 4. The energies are normalized such that the discrete-state potentials for the two models coincide. Note the diverse relative position of $V_0(R)$ and $V_d(R)$ in the two models, which leads to different magnitudes of the resulting DEA cross sections. Compared to the purely SEP+SE model, quantitative agreement of the calculated DEA rate constants with the experimental data of McCorkle *et al.* [5] is improved significantly in the final model. The shape of the DEA cross sections, however, remained nearly unaffected. Below 50 meV it is governed by the p-wave threshold behavior. Above 100 meV the cross section of DEA to the molecule in the ground rovibrational state decays exponentially (the exponents are 8.5 eV^{-1} for the SEP+SE model and 8.1 eV^{-1} for the improved one). The low sensitivity of the shape of the DEA cross sections to the exact shape of $V_0(R)$ or to the relative position of $V_0(R)$ and $V_d(R)$ is quite a surprising observation. We will postpone its discussion to Sec. IV.

In the present paper, all the cross sections have been obtained using the improved model. For numerical treatment of the nuclear dynamics the nonlocal resonance model is defined by cubic spline interpolation of the FN data for $V_0(R)$ and $V_d(R)$ for R varying from 2.5 to 20 bohr. For the discrete-state–continuum coupling we have used two-dimensional (in ϵ and R) cubic spline interpolation in the energy range from 0 to 10 eV and for internuclear distances between 2.5 and 6 bohr. The present model is limited to the electron energy up to 1.5 eV because of the presence of other

[1]Another reason is that restricted CI expansions are not suitable for R-matrix theory since the size inconsistency of the method violates the balance between the neutral (N-electron) and the scattering [$(N+1)$-electron] calculations.

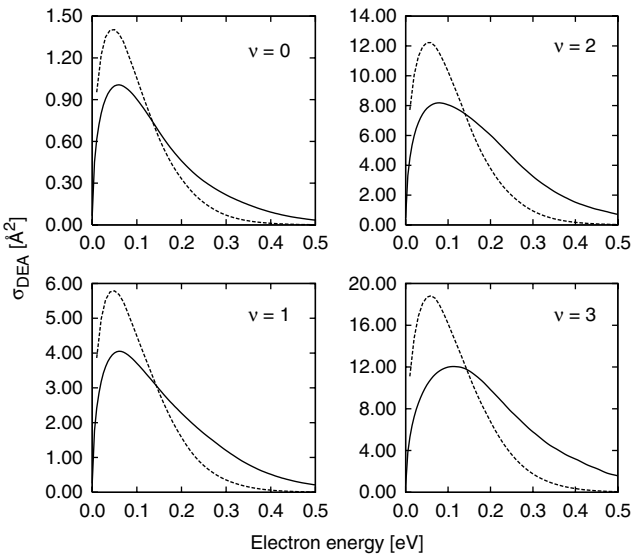

FIG. 5. Cross sections of DEA to the Cl_2 molecule in the lowest four vibrational states, $J=0$. Solid lines, present results; dashed lines, data from Ref. [7].

higher-lying resonances. The listed ranges of the electron energy and the molecular geometry are therefore sufficient to obtain converged cross sections and no extrapolation of the FN data is necessary. The Lippmann-Schwinger equation (2) with the nonlocal interaction Eq. (3) is solved using the Schwinger-Lanczos method [19] with only the lowest contributing angular momentum of the scattered electron ($l=1$) taken into account. For the Green's function $G_Q^{(+)}(E)$ the R-matrix representation described in [20] is used.

IV. DISSOCIATIVE ELECTRON ATTACHMENT

Figure 5 shows comparison of the calculated DEA cross section for the molecule in the lowest four vibrational states (angular momentum $J=0$) with the data obtained by Rut *et al.* [7]. In Fig. 6 the dependence of the DEA cross section on the rotational excitation of the molecule in the ground vibra-

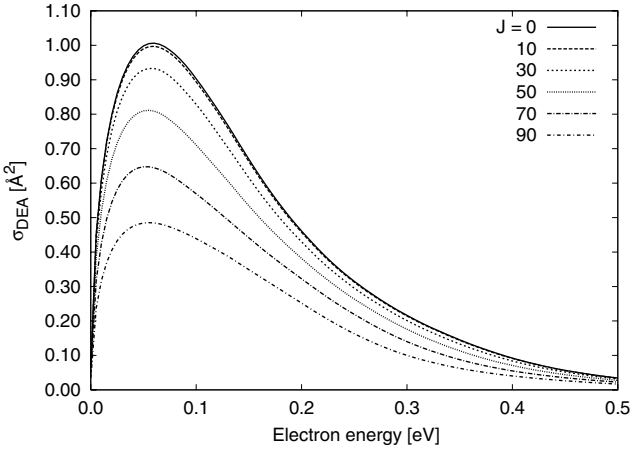

FIG. 6. Cross sections of DEA to rotationally excited molecules, $\nu=0$.

tional state is plotted. The shape of the DEA cross section σ_{DEA} depends only weakly on the vibrational excitation of the molecule. With increasing ν the maximum of σ_{DEA} moves slowly toward higher energies and the decay rate decreases. In the data of Rut *et al.* we observe even less sensitivity to the vibrational excitation. In contrast, the magnitude of σ_{DEA} depends strongly on the initial vibrational state ν of the molecule in both models. When the molecule is excited from its ground vibrational state to $\nu=1$ the cross section increases by a factor of 4 and $\sigma_{\mathrm{DEA}}(\nu=3)$ is nearly 12 times larger than $\sigma_{\mathrm{DEA}}(\nu=0)$. Compared to the data of Rut *et al.*, the present results are systematically smaller; the ratio at maximum is 0.72 for $\nu=0$ and 0.64 for $\nu=3$.

The rotational excitation has a much less pronounced effect on σ_{DEA}. Due to the large reduced mass of the chlorine molecule, the energy spacing between the rotational levels is very small, but even the excitation to high angular momentum J has only a minor influence on the cross section. Increasing J from 0 to 50 (which is energetically equivalent to the vibrational excitation from $\nu=0$ to 1 with $\delta E \approx 75$ meV) leads to a decrease of the magnitude of σ_{DEA} only by a factor of 0.81. The shape of the cross section peak is unchanged, both the position of the maximum and the rate of the decrease for higher energies. The low influence of the rotational excitation is caused by the shape of the centrifugal barrier in the interval of internuclear distances from 3.4 to 3.7 bohr. In this region the centrifugal barrier is flat and its only effect is an overall increase of the energy, both of the neutral molecule and of the Cl_2^- anion. The shape of the corresponding potential curves and their relative position, however, is changed negligibly and therefore the dynamics of the process is not significantly affected.

To better understand the observed dependencies we have investigated the process of DEA to Cl_2 on the basis of the general theory of dissociative attachment by O'Malley [36] using the approximation

$$\sigma_{\mathrm{DEA}} = \frac{\pi^2}{E}|F_{\mathrm{FC}}|^2 \Gamma(R_t)\exp(-\rho), \tag{13}$$

where F_{FC} is the Franck-Condon factor (FC), $\Gamma(R)$ is the adiabatic width, and R_t is the classical turning point of the final-state motion. The exponential is the so-called survival factor with the quantity ρ defined as

$$\rho = \int_{R_t}^{R_c} [\Gamma(R)/v_R(R)]dR, \tag{14}$$

where R_c is the crossing point of the neutral and the anion potential curves, and $v_R(R)$ is the classical velocity of the dissociating particles.

The growth of the DEA cross section with increasing vibrational excitation of the target (at least for the lowest few vibrational states) is general behavior observed in diatomic molecules. In the present case, the observed growth is fully supported by the theory of O'Malley, and we found it to be determined predominantly by the behavior of the FC factor. Decrease of the DEA cross section with increasing rotational excitation is, on the other hand, less usual behavior. It is determined by the character of the present model; the most important factor seems to be the position of R_c to the left of the equilibrium internuclear distance R_e of the neutral. With decreasing electron affinity (the crossing point moves toward R_e and beyond) the J dependence of the DEA cross section is eventually inverted (but not exactly when the crossing point coincides with R_e). As in the case of the vibrational excitation, the observed J dependence is in full agreement with the theory of O'Malley and is again governed by the behavior of the FC factor.

Comparison with experiment

There is only one absolute measurement of the cross section of DEA to Cl_2 by Kurepa and Belić from 1978 [3]. The energy resolution of the measurement was about 200 meV; the relative error of the measured cross section is claimed to be 20%. The gas temperature is not reported in the paper; we expect it to be close to the room temperature. The experiment found a peak at zero energy. The correct threshold behavior was revealed recently in a very accurate (energy resolution of about 3 meV) experiment by Ruf and co-workers [6,7], based on the laser photoelectron attachment method. In this experiment, relative values of σ_{DEA} were obtained in the energy range from 0 to 195 meV at a gas temperature around 500 K. McCorkle *et al.* [5] measured the DEA rate constants

$$k_{\mathrm{DEA}} = \sqrt{\frac{2}{\mu}}\int_0^\infty \sqrt{\epsilon}\sigma_{\mathrm{DEA}}(\epsilon,T)f(\epsilon,E/N,T)d\epsilon \tag{15}$$

as a function of mean electron energy $\epsilon_m=40-780$ meV for six temperatures between $T=213$ and 323 K. In Eq. (15), $f(\epsilon,E/N,T)$ is the electron energy distribution function in N_2 at the temperature T, and E/N is the density-reduced electric field.

In Fig. 7 temperature-averaged theoretical cross sections are compared with available experimental data. The threshold behavior of the cross section and the position of the peak maximum are correctly reproduced by the present theory in agreement with the data of Ruf *et al.* [7], but for energies above 80 meV the calculated cross section decreases slowly compared to the measurement. The temperature-averaged ($T=500$ K) cross sections calculated by Ruf *et al.* [7] are also shown in Fig. 7 (scaled to allow for better comparison of the shapes of the cross sections). Compared to present results the magnitude is by a factor of 1.4 larger and the cross section decays faster above 80 meV, following closely the experimental data. The measured DEA rate constants [5] are compared with our calculation in Fig. 8. The function $f(\epsilon,E/N,T)$ was approximated by the Maxwell-Boltzmann distribution. The theoretical rate constants peak at the energy about 100 meV for all temperatures, which is in good agreement with experiment. For higher energies the theoretical data decrease slowly, showing the deficiency of the present calculation we observed already in Fig. 7. The magnitude of the calculated rate constants agrees reasonably well with the data of McCorkle *et al.* The agreement deteriorates for low mean electron energies; see the comparison of the equilibrium (target gas and electron temperatures are equal) rate

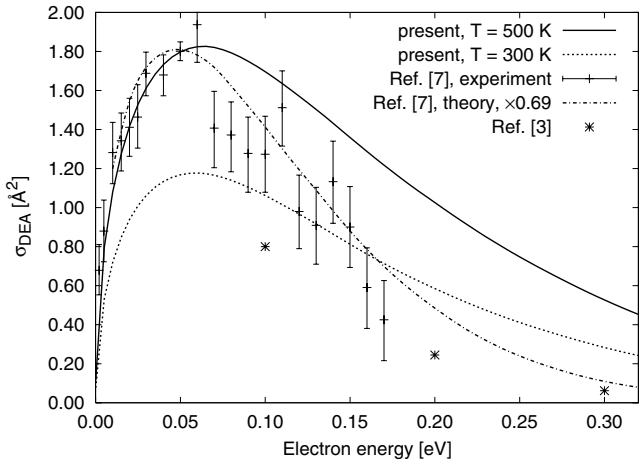

FIG. 7. Temperature-averaged theoretical cross sections σ_{DEA} for $T=500$ and 300 K are compared with the relative measurement of Ruf *et al.* [7] (scaled to fit present data for 500 K) and with the absolute measurement of Kurepa and Belić [3] (asterisks). The value $\sigma_{\mathrm{DEA}}=2.02$ Å^2 at zero energy [3] is out of the range of the figure. Also shown are theoretical data obtained from the semiempirical single-pole R-matrix theory (dash-dotted line, scaled to fit magnitude of present data).

constants in Table I ($T=253$ K corresponds to a mean electron energy about 33 meV). In this range the calculated rate constants decrease faster than indicated by the experiment. A similar comparison between the data of McCorkle *et al.* and the single-pole R-matrix theory of Fabrikant *et al.* can be found in Ref. [8]. In correspondence with the observations made in Fig. 7 the agreement is better than in the present calculation, considering both the magnitude and shape of the rate constants.

In the present model, the relative position between the neutral and anionic potential curves is determined rather equivocally. In the SEP approximation the treatment of the neutral and anionic systems is clearly unbalanced. In the improved model, the use of electron affinity to determine the relative position in the asymptotic region might not lead to entirely correct results for small internuclear distances. To determine whether the disagreement between our results and

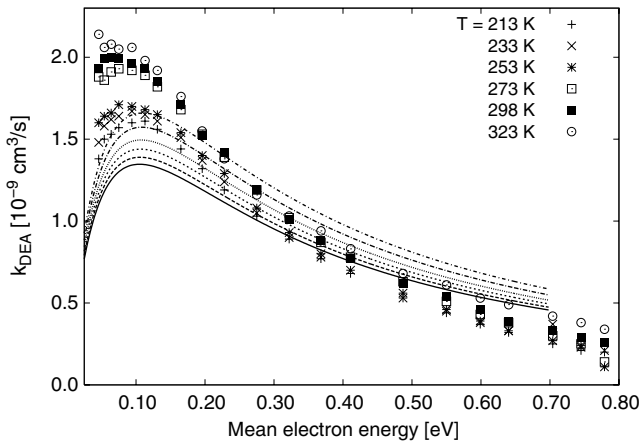

FIG. 8. DEA rate constants measured by McCorkle *et al.* [5] (points) compared with the present theory (lines).

TABLE I. Equilibrium DEA rate constants obtained from the swarm experiment of McCorkle *et al.* [5] and from the present theory. Measured rate constants are listed in the second column and calculated ones in the third column. The last column shows the ratios between the experimental and theoretical values.

T (K)	Experiment (10^{-9} cm^3/s)	Theory (10^{-9} cm^3/s)	Ratio
213	1.22	0.82	1.49
233	1.35	0.90	1.50
253	1.51	0.97	1.56
273	1.67	1.06	1.58
298	1.86	1.16	1.60
323	2.14	1.27	1.68

the experimental data is caused by this uncertainty we have analyzed the dependence of the cross section (in particular, its decay rate for energies above 100 meV) on the electron affinity in the range between 3.1 and 3.7 eV. Our calculations showed that the rate of the decay varies only within 10% around the average value in the studied range of electron affinity, which cannot explain the observed discrepancy. On the other hand, the magnitude of the DEA cross sections depends strongly on the electron affinity. Therefore, the good agreement of the calculated rate constants with the data of McCorkle *et al.* supports the use of electron affinity to determine the crossing point of $V_0(R)$ and $V_d(R)$.

Similar observations can be made on the basis of the theory of O'Malley. The relative position of neutral and anionic potential curves affects drastically the magnitude of the Franck-Condon factor, but its decay rate changes only within 15% around the average value. The same holds true also for the cross sections determined from Eq. (13), even though the decay rate of σ_{DEA} is significantly affected also by the resonance width and the survival factor. We conclude that the shape of the DEA cross secton is predominantly determined by the shape of the resonance width function and by the slope of $V_d(R)$ in the resonance region. The principal deficiency of present calculations and the disagreement with experimental data originates in low level of correlation taken into account in FN calculations rather than in the wrong position of the crossing point R_c.

V. VIBRATIONAL EXCITATION

In this section we give a brief survey of the cross sections σ_{VE} of the vibrational excitation. Cross sections of VE from the ground and first excited vibrational states to several final states are plotted in Fig. 9. The dependence of σ_{VE} on the rotational excitation is analyzed in Fig. 10 on the example of channels $0\rightarrow1$ and $0\rightarrow3$. We observe that in all plotted channels σ_{VE} peaks at about the same collision energy 400 meV. With increasing excitation the increase of the threshold is steeper and the peak narrows. As in the case of DEA the dependence of the cross sections on the angular momentum J is rather weak. With increasing J the magnitude

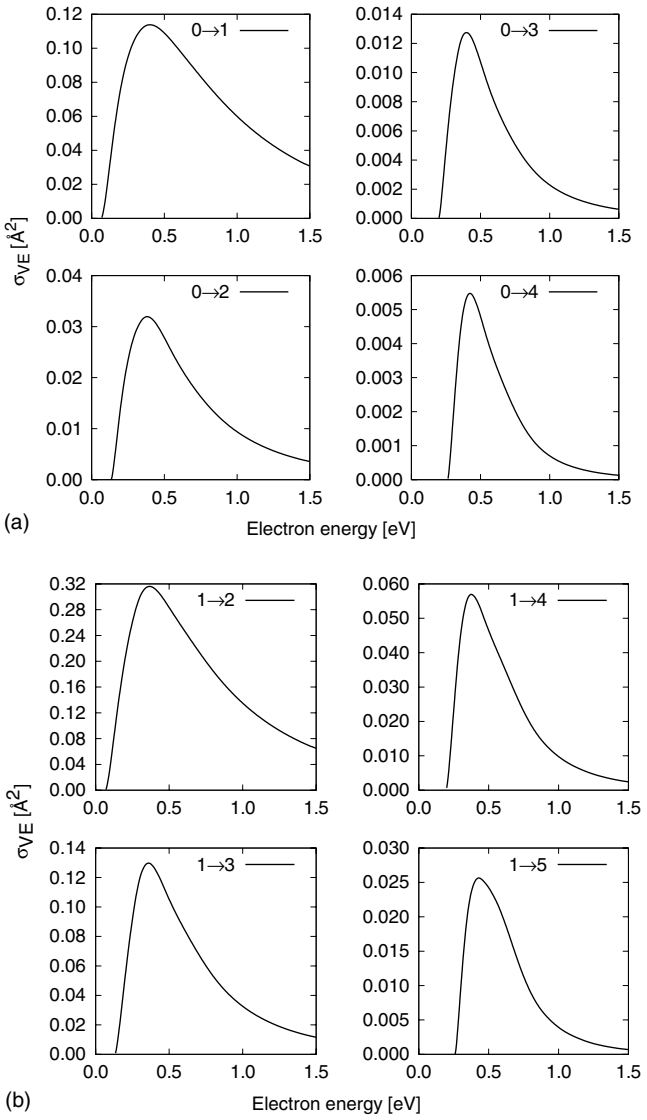

FIG. 9. VE of the Cl_2 molecule.

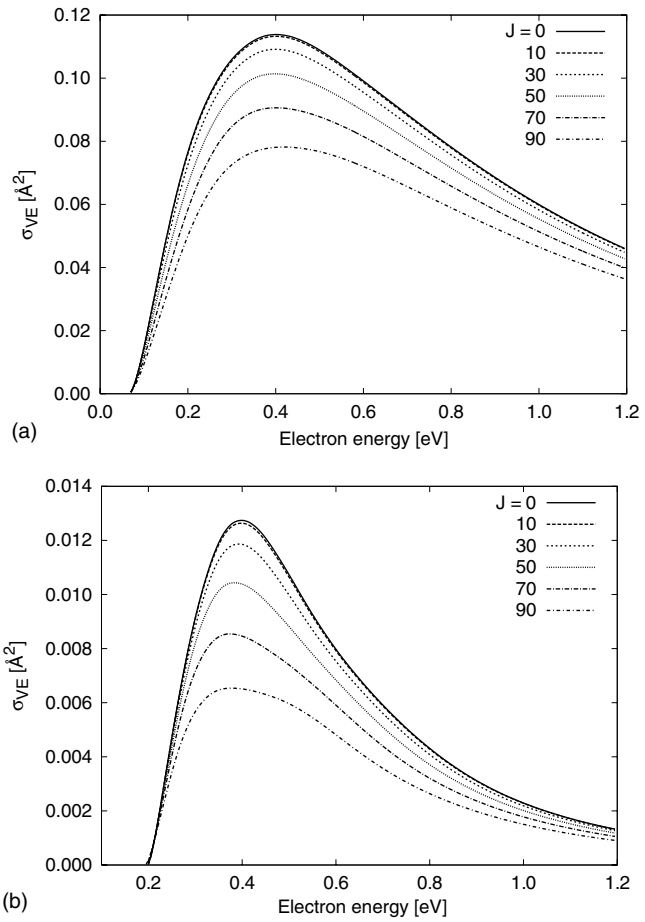

FIG. 10. Dependence of the VE $0\rightarrow1$ and $0\rightarrow3$ cross sections on the rotational excitation.

of the cross sections decreases slowly, and the shape is not changed noticeably.

Figure 11 shows the comparison of the present calculations with the single-pole *R*-matrix theory of Fabrikant and co-workers [7,8]. We observe that there is a fundamental disagreement in both the magnitude and the shape of the cross sections. The magnitude of σ_{VE} obtained by the present model is significantly smaller in channels $0\rightarrow1$ or $1\rightarrow2$, but it decreases more slowly with increasing final vibrational state ν_f. As a result the magnitudes determined by the two calculations agree in channels $0\rightarrow3$ and $1\rightarrow3$. In channel $0\rightarrow4$ the present model yields even larger cross sections than the calculation of Fabrikant *et al.* Also the shapes of the peaks are completely different in both theories. In the present model, the maximum is more pronounced, located at the same energy independent of the particular channel of VE, which is not the case of the single-pole *R*-matrix theory. Beyond the maximum, cross sections calculated in the framework of the NRM decay exponentially with much smaller rate than the cross sections of Fabrikant and co-workers, which drop suddenly toward zero at energy about 1 eV. At present, the reasons for such a deep disagreement between the two theories are unclear to the authors.

As stated in the introduction, the experimental data on VE of Cl_2 are strongly limited; no direct measurements have been carried out so far. Rough estimates of the total VE cross section derived from the difference of the total inelastic electron scattering cross section and total ionization and dissociation cross sections, for which experimental data are available, are provided by Christophorou and Olthoff [1]. Other predictions have been made on the basis of Boltzmann-code calculations using data from swarm experiments [9,10]. Below 1 eV, the magnitudes of the total VE cross sections predicted in these works vary between 1 and 3 $Å^2$, favoring the calculation of Fabrikant *et al.* over the present model. The calculations of Rogoff *et al.* and Pinhão and Chouki exhibit one broad peak extending from threshold an the energy between 4 and 6 eV, which is in disagreement with the cross section estimated by Christophorou and Olthoff. The latter exhibits two peaks and loosely resembles the data of Fabrikant *et al.*, though the sudden drop of the low-energy peak (corresponding to the $^2\Sigma_u^+$ resonance) occurs at somewhat higher energy around 2 eV. Also, the second peak in the energy range of the $^2\Pi_g$ and $^2\Pi_u$ resonances (the present model does not describe this energy range) is significantly displaced compared to the calculation of Fabrikant *et al.* At

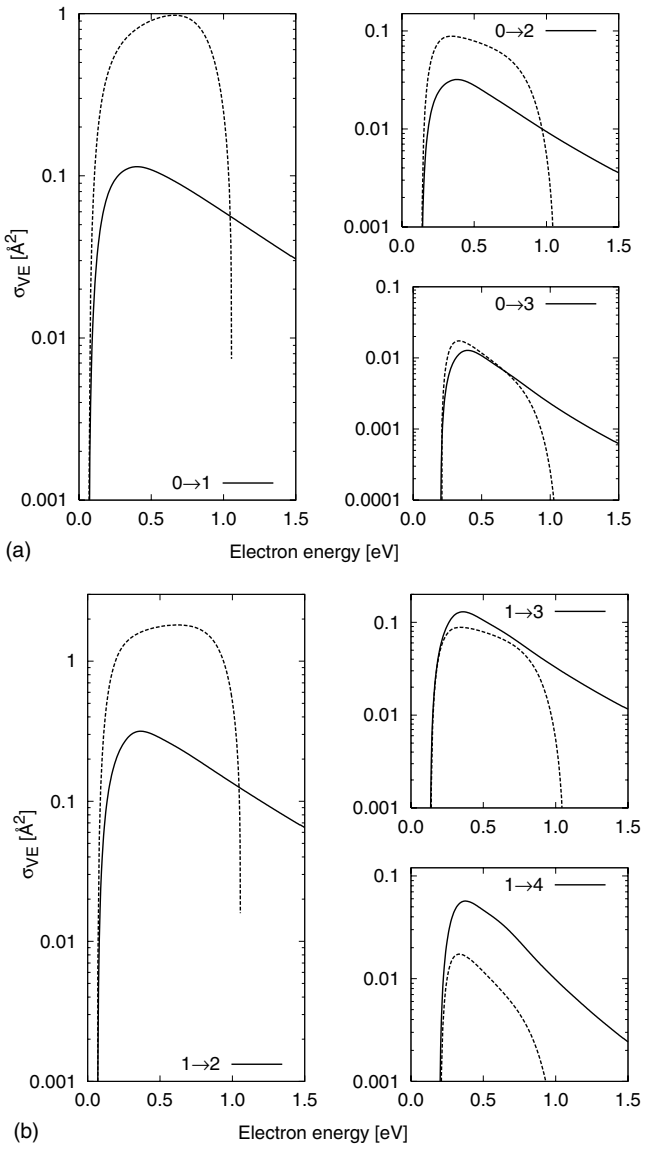

FIG. 11. Comparison of the VE cross sections determined by the present model (solid lines) with the single-pole *R*-matrix theory [7] (dashed lines).

the present time the experimental data cannot give conclusive support for either of the two calculations owing to their limited reliability as well as to considerable disagreements with the calculations.

VI. CONCLUSIONS

In the present work the recently developed Feshbach-Fano *R*-matrix methodology [25,29,30] was used to construct a nonlocal resonance model of the $^2\Sigma_u^+$ resonance in low-energy electron-Cl_2 collisions. The model was used to obtain cross sections of the processes of dissociative electron attachment and vibrational excitation.

The FFR approach is based on the fixed-nuclei *R*-matrix calculations. The discrete component of the Hilbert space, associated with the resonance, is expanded in terms of the *R*-matrix basis and is extracted from the background scattering subspace. In the present application the FFR methodology was able to extract the $^2\Sigma_u^+$ resonance correctly for all internuclear distances, resulting in background scattering eigenphases that are only weakly dependent on both the collision energy and the internuclear distance. The acquired discrete state and the background continuum states are therefore good candidates to form a diabatic electronic basis suitable for the treatment of the nuclear dynamics of the resonant collisions. The *R*-matrix calculations were carried out at the static-exchange plus polarization level of theory. To improve the model, the potential of the neutral molecule and the discrete-state potential in the bound-state region were recalculated at the MRD-CI level to obtain correct asymptotic behavior of the potential curves and to improve the relative position of the energies of neutral and anionic systems, making use of the accurate value for the electron affinity of chlorine. The inconsistency of the bound-state and scattering calculations, however, represents a serious drawback of the present model. New calculations utilizing advanced *R*-matrix codes allowing for higher levels of correlation are desirable.

For the process of DEA, the present model yields cross sections that exhibit correct threshold behavior in agreement with the latest experiment [7], but at higher collision energies the calculated cross sections decrease slowly. We attribute this deficiency to the low level of electron correlation taken into account in the fixed-nuclei *R*-matrix calculations. The shape of the cross sections is predominantly determined by the shape of the resonance width function and by the slope of the discrete state potential in the resonance region. Our analysis showed that the shape of σ_{DEA} is rather insensitive to the exact shape of $V_0(R)$ or to the relative position of the potential curves of Cl_2 and Cl_2^- (for electron affinities within the range of 600 meV around the exact value 3.42 eV). The use of the more accurate MRD-CI potential curves, however, improved significantly the magnitude of the calculated cross sections, which is extremely sensitive to the relative position of the two potential curves. The rate constants derived from the present calculations agree reasonably well with the measurement of McCorkle *et al.* [5].

Concerning the process of VE, the present calculations are in complete disagreement with the data published in Refs. [7,8], based on the single-pole *R*-matrix approximation. The rough estimates of the total VE cross section based on indirect experimental data are slightly in favor of the semiempirical theory of Fabrikant *et al.*, but significant disagreement between the experiment and theory and between the experimental data themselves prevent us from making any conclusions concerning the reliability of the two theoretical calculations.

It should be stressed again that the inaccuracy of the cross sections yielded by the present model is rather due to the inadequate representation of the electronic wave function in the fixed-nuclei calculations than due to the failure of the FFR method. The methodology itself represents particularly valuable approach to the problem of diabatization of the electronic basis. In principle, it can provide several equiva-

lent separations of the Hilbert space into resonance and background scattering parts (the discrete state is not defined unambiguously in the Feshbach-Fano formalism), which can be extremely useful if we want to assess the stability and reliability of the calculations based on the nonlocal resonance model.

ACKNOWLEDGMENTS

The authors are thankful to B. M. Nestmann and V. Brems for useful discussions. This work was supported by the Grant Agency of the Academy of Sciences of the Czech Republic grant No. IA100400501 and by EIPAM.

[1] L. G. Christophorou and J. K. Olthoff, J. Phys. Chem. Ref. Data **28**, 131 (1999).
[2] W.-C. Tam and S. F. Wong, J. Chem. Phys. **68**, 5626 (1978).
[3] M. V. Kurepa and D. S. Belić, J. Phys. B **11**, 3719 (1978).
[4] R. Azria, R. Abouaf, and D. Teillet-Billy, J. Phys. B **15**, L569 (1982).
[5] D. L. McCorkle, A. A. Christodoulides, and L. G. Christophorou, Chem. Phys. Lett. **109**, 276 (1984).
[6] S. Barsotti, M.-W. Ruf, and H. Hotop, Phys. Rev. Lett. **89**, 083201 (2002).
[7] M.-W. Ruf, S. Barsotti, M. Braun, H. Hotop, and I. I. Fabrikant, J. Phys. B **37**, 41 (2004).
[8] I. I. Fabrikant, T. Leininger, and F. X. Gadéa, J. Phys. B **33**, 4575 (2000).
[9] G. L. Rogoff, J. M. Kramer, and R. B. Piejak, IEEE Trans. Plasma Sci. **PS-14**, 103 (1986).
[10] N. Pinhao and A. Chouki, in *Proceedings of the XXII International Conference on Phenomena in Ionized Gases, Hoboken, NJ, 1995*, edited by W. E. Carr, K. Becker, and E. Kunhardt, pp. 5–6.
[11] W. Domcke, Phys. Rep. **208**, 97 (1991).
[12] M. Čížek, J. Horáček, and W. Domcke, Phys. Rev. A **60**, 2873 (1999).
[13] M. Čížek, J. Horáček, A.-C. Sergenton, D. B. Popović, M. Allan, W. Domcke, T. Leininger, and F. X. Gadea, Phys. Rev. A **63**, 062710 (2001).
[14] M. Čížek, J. Horáček, M. Allan, I. I. Fabrikant, and W. Domcke, J. Phys. B **36**, 2837 (2003).
[15] H. Feshbach, Ann. Phys. **5**, 357 (1958).
[16] H. Feshbach, Ann. Phys. **19**, 287 (1962).
[17] U. Fano, Phys. Rev. **124**, 1866 (1961).
[18] M. Čížek, Ph.D. thesis, Charles University in Prague, 1999 (unpublished).
[19] H. D. Meyer, J. Horáček, and L. S. Cederbaum, Phys. Rev. A **43**, 3587 (1991).
[20] P. Kolorenč, M. Čížek, J. Horáček, G. Mil'nikov, and H. Nakamura, Phys. Scr. **65**, 328 (2002).
[21] W. Domcke and C. Mündel, J. Phys. B **18**, 4491 (1985).
[22] A. U. Hazi, J. Phys. B **11**, L259 (1978).
[23] A. U. Hazi, C. Derkits, and J. N. Bardsley, Phys. Rev. A **27**, 1751 (1983).
[24] M. Berman and W. Domcke, Phys. Rev. A **29**, 2485 (1984).
[25] B. M. Nestmann, J. Phys. B **31**, 3929 (1998).
[26] T. Beyer, B. M. Nestmann, and S. D. Peyerimhoff, J. Phys. B **33**, 4657 (2000).
[27] T. Beyer, B. Nestmann, and S. Peyerimhoff, J. Phys. B **34**, 3703 (2001).
[28] B. M. Nestmann, S. V. K. Kumar, and S. D. Peyerimhoff, Phys. Rev. A **71**, 012705 (2005).
[29] V. Brems, T. Beyer, B. M. Nestmann, H.-D. Meyer, and L. S. Cederbaum, J. Chem. Phys. **117**, 10635 (2002).
[30] P. Kolorenč, V. Brems, and J. Horáček, Phys. Rev. A **72**, 012708 (2005).
[31] P. G. Burke and K. A. Berrington, *Atomic and Molecular Processes: An R-matrix Approach* (IOP Publishing, Bristol, 1993).
[32] C. Bloch, Nucl. Phys. **4**, 503 (1957).
[33] D. E. Woon and J. Thom H. Dunning, J. Chem. Phys. **98**, 1358 (1993).
[34] B. M. Nestmann and S. D. Peyerimhoff, J. Phys. B **23**, L773 (1990).
[35] S. D. Peyerimhoff and R. J. Buenker, Chem. Phys. **57**, 279 (1981).
[36] T. F. O'Malley, Phys. Rev. **150**, 14 (1966); **156**, 230(E) (1967).